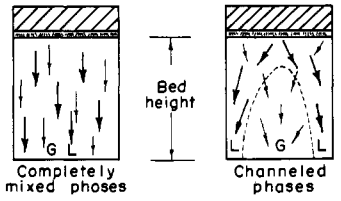

Figure 17. Flow patterns within co-current packed beds

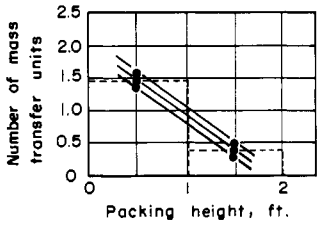

Figure 18. Mass transfer units *vs.* packing height

bed, this assumption would be correct. However, a visual observation of the flow patterns indicates an accumulation of the liquid phase near the wall after passage through about 1 foot of the packing. An explanation of this pattern would be a tendency of the higher gas rates to force the liquid into the annulus channel near to the wall surrounding the gas channels moving down the center of the column. This channeling would reduce the interphase turbulence as the phases move down the bed, decreasing the interfacial surface area, a, and thus would decrease the mass transfer coefficient $K_H a$. This separation of the phases was illustrated in Figure 17.

The reduction in the mass transfer rate with respect to column height was indicated in Figure 18, showing the number of mass transfer units exchanged in each foot of a 2-foot bed of ¼-inch Raschig rings with constant gas and liquid mass rates.

The comparatively greater interphase turbulence at the entrance portion of the bed producing a greater mass transfer would produce a skewed form of the operating-equilibrium curves than the curves assumed by the log-arithmic mean driving force.

LITERATURE CITED

(1) Collins, D.E., Ph.D. dissertation, Prudue University, Lafayette, Ind. 1958.
(2) Dodds, W.S., Ph.D. dissertation, Northwestern Univ., Evanston, Ill. 1953.
(3) Dodds, W.S. Stutzman, L.F., Sollami, B.J., R.J. McCarter, *A.I.Ch.E. J.* **6**, 197, 1960.
(4) Leva, Max, United States Stoneware Co., Akron, Ohio, Bull. TP 54, 1951.
(5) McIlvriod, H.G., Ph.D. dissertation, Carnegie Inst. Technol., Pittsburgh, Pa., 1956.

RECEIVED for review April 23, 1962. Accepted August 24, 1962.

Material supplementary to this article has been deposited as Document No. 7378 with the ADI Auxilliary Publications Project, Photoduplication Service, Library of Congress, Washington 25, D. C. A copy may be secured by citing the document number and by remitting $1.25 for photoprints or $1.25 for 35-mm. microfilm. Advance payment is required. Make checks or money orders payable to Chief, Photoduplication Service, Library of Congress.

Pressure Drop Through Packed Beds Operated Cocurrently

C. Y. WEN, WILLIAM S. O'BRIEN,
West Virginia University, Morgantown, W. Va.

LIANG-TSENG FAN,
Kansas State University, Manhattan, Kan.

This article provides pressure drop data through packed towers under cocurrent operation and by use of the following packings: 1/4-inch Raschig rings, 1/2-inch Raschig rings, 1/2-inch Berl saddles, 1/2-inch Intalox saddles, 1-inch Raschig rings, and 1-ich Intalox saddles. A correlation for the continuous gas phase-dispersed liquid phase region is empirically presented. Constants are obtained for each packing, as well as for different fluid properties; therefore, this form cannot be directly extended into other packing or fluid systems without further investigations. However, the data fit the empirical formula well.

THE COMMON OPERATION of packed columns has been the countercurrent operation (*4*); however, cocurrent operation can be advantageously employed in some cases (*7*). This article provides pressure drop data through packed towers under cocurrent operation.

The first collection of pressure drop data over a packed bed with a cocurrent system was done by Dodds (*1*). Using 1-inch and 1.5-inch Berl saddles and Intalox saddles, and 2-inch steel rings as packing meterial in an 18-inch diameter column, the author measured the cocurrent pressure drop and holdup of two systems air-water and air-2.5N Na_2CO_3 (liquid density, 1.12). The mass rates measured were: liquid range, 4250 to 33,350 lb./sq. ft. hr. and air range, 197 to 1810 lb./sq. ft. hr. Dodds did not correlate the data, but only presented it in tabular and graphical form as a reference. In 1960 article, he and co-authors presented the data for both pressure drop and liquid holdup in a graphical form (*2*).

The first correlation for the cocurrent pressure drop in packed beds was presented by McIlvriod (*6*). With a 2-inch diameter column packed with 4-mm. and 6-mm. glass beads and 1/4-inch Raschig rings, liquid flow rates from 7080 to 94,350 lb./sq. ft. hr. and gas mass rates from 400 to 4000 lb/sq. ft. hr. were investigated. The height of packing was varied with a maximum height of 4.50 inches. The pressure drop data were plotted on log-log coordinate paper resulting in two distinct zones. The lower zone was an unsteady pulsating flow occurring at low gas to liquid ratios. At higher gas to liquid ratios, another zone existed which was divided into three regions. A break point existed in the pressure drop *vs.* gas rate curve using constatn liquid rates as the parameter. The three regions defined were liquid

rates below the column flooding point, liquid rates above the flooding point and gas rates below the break point, and liquid rates above the flooding point and the gas rates above the break point.

Three types of empirical correlations were presented and discussed. The first correlation was the type offered by Martinelli (5) for cocurrent flow in open pipes. As good a success was achieved for horizontal open pipes, but as much as 80% deviations were obtained, particularly in the region of low gas rates.

The second correlation presented was derived semi-empirically by the author in the form

$$\frac{(\Delta P g_c/z)_{TP}}{(\Delta P g_c/z)_G} = \phi_G^2 = 1 + \beta \frac{L}{G^{1+m}}$$

with two experimental constants, β and m, which must be determined for the three regions listed above. The equations obtained fitted the data for the three packings within $\pm 15\%$ accuracy, but the difficulty was in identifying the exact flow region for the corresponding rates.

The third correlation used a modified friction factor concept. The friction factor was defined as:

$$\frac{(\Delta P g_c/z)_{TP} D_p \rho_G^2}{2\rho_{avg} G^2}, \text{ with } \rho_{avg} = \frac{G+L}{G+(\rho_G/\rho_L)L}\rho_G$$

The resultant curve of f' *vs.* a particle Reynolds number, (D_pG/μ_G), was of the typical friction factor shape, branching at higher Reynolds numbers with various liquid rates.

The most elaborate investigation of cocurrent two-phase pressure drop was done by Larkins (3). The tests were made with 3/8-inch Raschig rings, 3/8-inch spheres, and 1/8-inch cylinders, 4 inches in diameter, 7 feet in length of transparent plastic pipe. With air as the gas phase, the effects of various liquid properties were examined, using liquid phases: water, ethylene glycol, 2.5 weight % methyl-cellulose solution, and a mildly foaming soap solution. The phase rate ranges are: liquid phase, 4000 to 216,000 lb./ sq. ft. hr.; gas phase, 50 to 1200 lb./sq. ft. hr.

The equipment was arranged with a pair of quick-closing valves located directly above and below the packed section featuring a unique lever mechanism to close the two valves simultaneously and enable an accurate measurement of the liquid holdup within the packed section. However, in an attempt to eliminate all void space between the valves and thus measure only the holdup within the packing, the packing, the packing was placed as close to the bottom valve as physically possible. Holdup data showed, in all cases, a 100% saturation of packing void spaced with liquid for all of the liquid flows with zero gas flows. While the resistance of the bed may produce the 100% saturation, the presence of the valve directly below the packing may cause an induced holdup. The column was divided into three sections for pressure drop measurement. In almost all cases, the middle section showed the least pressure drop per packing length, the top section a slightly higher pressure drop, but the bottom section pressure drop was the highest. Thus, the larger pressure drop in the bottom section might be due to the induced holdup collecting directly above the valve. There is no way to determine the effect of the added resistance, but the discrepancy seems to be apparent. The accuracy of Larkin's experimental data was given as a standard deviation of 6.6% for the pressure drop data and a deviation scatter of +55% to −30% for the holdup relationship.

Flow through packed beds presents an energy loss due to the obstructions in the flow path in addition to the frictional energy loss. The continual reversing of the linear flow path as it picks its path down the column and also the continual expansion and contraction of a compressible fluid will cause an additional energy loss.

When the packed column is operated as a two-phase countercurrent contacting device, the region of operating capacity is limited by the flooding point. A brief explanation of the flooding phenomenon in relation to liquid holdup and pressure drop might aid in the understanding of the flow patterns within the bed.

With low liquid and low gas rates in a countercurrent flow system, the liquid passing down over the packing falls as independent flow and is affected very slightly by the opposing upward gas flow. From the standpoint of the gas flow, the falling liquid is an inert body and can be treated with the packing particles as an obstruction unit met in the gas passage up through the bed. As the liquid flow rate is increased, more liquid is retained in the packed bed. Thus, the energy necessary to force the gas stream upward through the packing, the pressure drop, is increased by the reduction of the cross-sectional flow area caused by the higher liquid rates. The pressure drop correlation with the gas rate can expect to follow the single-phase gas rate mechanism with the liquid rate only indicating a reduction in the gas flow area. The empirical relationship for the countercurrent bed operation indicates this mechanism, with the pressure drop data correlating with the second power of the gas flow rate, taking the form

$$\Delta P = \alpha 10^{\beta L} G^2 \qquad (1)$$

The constants evaluated as a function of the properties of the fluids and the packing particles.

Nearing the flooding point of the column, that combination of liquid and gas flow rates at which the column plugs up and ceases to operate, the liquid holdup has filled the column to such an extent that the gas must force its way up through the liquid. This short region of gas rates in which the gas flow requires greater energy than normal to force its way is known as the loading zone. A slight liquid rate increase will produce the point at which the gas can no longer force a path through the liquid, and the operation ceases to function.

The cocurrent two-phase flow downward through packing has not previously been investigated insofar as correlating the pressure drop of the bed with the flow rates of the phases is concerned. The previous work in either packed beds or open pipes equated the two-phase pressure drop as a function of the estimated pressure drop of either phase if that phase were flowing alone in the column.

The original premises made my Martinelli, and others (5) with his correlation stated that the flow was homogeneous with the pressure drop of the liquid phase equaling the pressure drop of the gas phase, with no plug flow or no radical pressure drop differences; the void space filled by the liquid phase plus the void space filled by the gas phase equals the total void space of the flow path of the coumn. In a generalized analysis of the possible flow patterns of the fluids in a cocurrently operating packed bed, these requirements would only be attained when the phases were moving down the column at large enough flow rates to totally mix the streams into a homogeneous single pseudo-phase.

At low liquid and gas rates, the flow is channeled without the necessary turbulence to mix the two phases into a homogeneous pseudophase. Also with irregularly shaped packings, moderately inactive void spaces free of liquid can be expected to form on the leeward side of the packing from the flow direction with low liquid flow rates. The relationship of pressure drop with gas rate for this region would be hard to predict since the correlation would depend upon the ability of the two-phase distributor on top of the packing to provide an even distribution of the phases. Generally, by the nature of the phases, the liquid phase with very low liquid rates would tend to trickle over the packing into flow channels, the higher gas phase stream by passing the liquid stream.

As the gas rate is increased, a certain ratio of gas rate to liquid rate is reached at which the liquid is vitually dispersed into the gas, forming a uniform mixture. There is very little or no slippage between the continuous phase and the dispersed phase. Thus, the pressure drops in this region could be related in terms of the mixture flow rate and the mixture density as if the system were a single-phase flow.

The locations of these regions (Figure 1) represent data obtained in preliminary test runs. This particular set of data was obtained with a water-air ssystem through a glass column 4 feet in height and 4 inches in diameter, packed with 1/4-inch carbon Raschig rings.

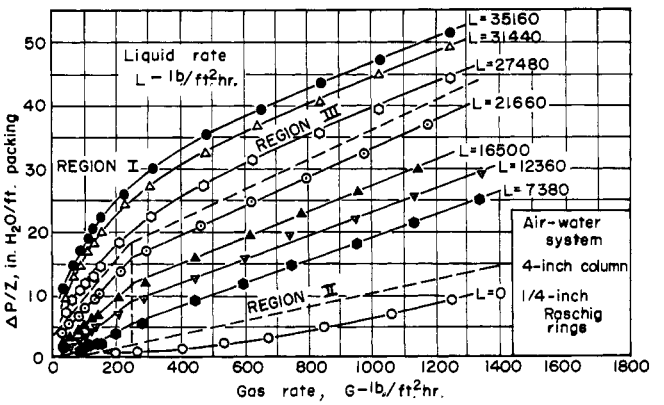

Figure 1. Two-phase pressure drop; theoretical flow regions

The first or channeled-flow region exists, for this set of data, for the low gas flow rates up to a transition range located in the gas mass rate region of 150 to 250 lb./sq. ft. hr. The relationship of the pressure drop *vs.* gas rate curves for low liquid rates follows the pattern of the zero liquid rate curve; the pressure drop varied as approximately G^2, indicated an independence of the gas flow with the liquid stream. The effect of the increasing liquid rate only reduced the flow area of the gas stream.

At higher gas flow rates Region II exists, in which a different relationship of the pressure drop and the mass flow rates is indicated. Within this region the flow mechanism can be assumed to be a thoroughly dispersed liquid phase throughout the continuous gaseous phase.

Region III exists at high liquid rates and visually suggests a single relationship for the complete gas rate range. The mechanism of this region might also be a dispersed phase flow, but because of the high liquid rate to gas rate ratio, the liquid phase can be assumed to be the continuous phase with the gas phase completely dispersed throughout the liquid.

The approximate power function of the gas mass rate with its effect on the pressure drop can be visualized: Region I. The power function of G varies from 2.0 at very low liquid rates to a fractional value at higher liquid rates. Region II. ΔP varies approximately linearly with G. Region III. The power of G seems to be less than unity with possible variation.

Zero and Lower Liquid Rates: ΔP varies approximately as G^2. The exponents of G would have to be investigated for the regions as well as the physical boundaries of the regions.

While measuring the pressure drop of the two phases, two hard rubber gaskets were placed at the top and bottom of the packed sections. The pressure-drop probes were 1/4-inch copper tubes passing through holes bored in the gaskets with the tube ends flanged.

By a system of copper tubing, 1/4-inch steel pipes, and rubber tubing, the probes were connected to a bank of four manometers containing different fluids, allowing more accurate differential pressure readings by a variety of liquid densities. The manometers were connected in parallel with rubber tubing provided with pinch clamps to close off any manometer, should its pressure range be exceeded. The manometers were three vetical U-tubes containing distilled water, sp. gr. = 1.000; *s*-tetrabromoethane, sp. gr. = 2.9638; mercury sp. gr. = 13.546, and one U-tube slanted at an angle of 11°27′ filled with distilled water.

EXPERIMENTAL PROCEDURE

The equipment packings used in this work are described in the previous article (7).

The pressure drop data were recorded for combinations of eight liquid rates and eleven gas rates, including the zero gas rate.

The concentration of the calcium chloride solution did not change significantly during the operating time, thus the concentration was only measured periodically and averaged for the entire set of runs for the particular packing type.

DISCUSSION

The pressure drop data are presented in Figures 2 to 7. The constant liquid rate curves were quite similar in form to those illustrated in the previous section and were also similar to the results of other investigators.

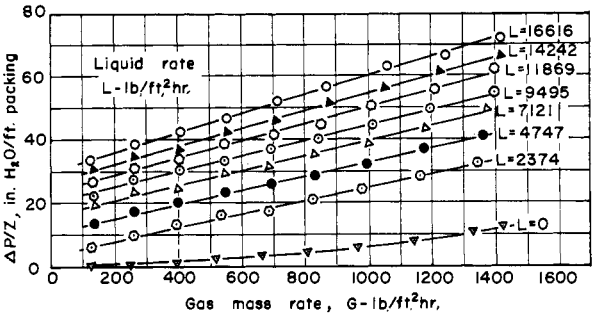

Figure 2. Pressure drop data; ½-inch Raschig rings

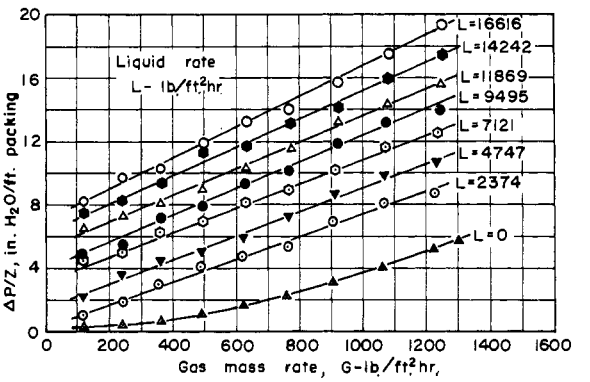

Figure 3. Pressure drop data; ½-inch Raschig rings

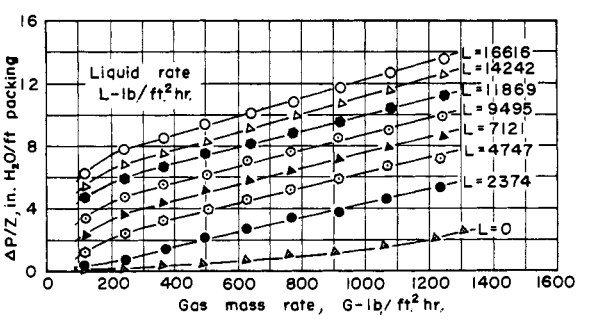

Figure 4. Pressure drop data; ½-inch Berl saddles

Two of the three regions described in the pressure drop and flow region seem to be indicated by the experimental results. The continuous gas phase region, Region II, was in evidence in the data of each of the six packing types. The channeled flow region, Region I, was indicated in the data curves of the larger packing for lower gas rates. The third region was not in evidence because of the low range of liquid flow rates investigated.

No attempt was made to obtain a correlation in Region I because of the probable experimental error and few data points lying within this region. In this region, the bed and packing configuration, the efficiency of the two-phase distributior, and the flow pattern of the phases all have a great effect on the pressure drops.

A correlation for the continuous gas phase–dispersed liquid phase region has been empirically presented as

$$\Delta P = a(L - b)^c + d\ 10^{eL}G \qquad (2)$$

The constants a, b, c, d, and e must be evaluated for each packing, as well as for different fluid properties; therefore, this form cannot be directly extended into other packing or fluid systems without further investigations. However, the data fit the empirical formula well.

The constants evaluated for the six types of packing for the continuous gas phase region are presented in Table II. The equation is presented with ΔP, G, and L expressed in the dimensions indicated.

The assumption was made that within this particular region, the gas and liquid phases were completely mixed to form one homogeneous phase; variations in the gas and liquid rates serve only to vary the physical properties of the phase. With this assumed flow pattern, the original Martinelli (5) two-phase flow premise can be assumed correct: that the pressure drop of the gas phase equals the pressure drop of the liquid phase rate over the length of flow path. Therefore, as either the gas or the liquid phase rate approaches zero, the pressure drop correlation should reduce to a function of the flow rate of the other phase rather than zero. The first term of Equation 2 must be assumed zero when L is less than g, and c is a fraction.

The accuracy of the correlation was quite good, especially for the ¼-inch and the ½-inch particle sizes. The ¼-inch size correlates remarkably well with an average deviation of ± 1.7% and with 90% of the data correlating within the maximum deviation range of ± 4%. The larger deviations of the data with the 1-inch packing could be attributed to a large packing size to bed diameter ratio and an instability of the formation of the flow range pattern at the lower liquid rates.

The relationship of the constants with other factors affecting the pressure drop are not known. The pressure drop is believed to be inversely proportional to the size of the packing particles, but the factors due to the changing particle size, such as spherisity, void space, surface area, and packing arrangement are not known. The physical properties of the phases naturally affect the pressure drop and liquid holdup within the bed. The effects of these factors are interrelated in the resultant pressure drop and must be investigated individually before a correlation can be made.

The variation of the flow pattern with bed height, indicated by the mass transfer investigation, would greatly affect the pressure gradient of the bed. The phase separation would produce a radial variation of the pressure drop, similar in analysis to stratified flow with the two-phase flow in open channels, and would produce a lower pressure differential than would be produced in a completely homogeneous flow. The effect of bed height on the pressure drop was not studied in this investigation.

Previous two-phase flow investigators have separated the flow patterns into various regions by visual breakpoints in the pressure drop–gas rate plots on logarithmic

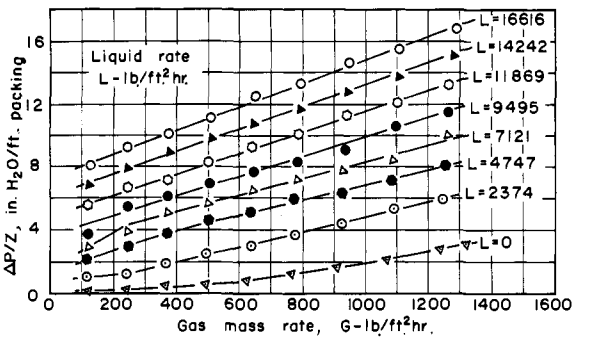

Figure 5. Pressure drop data; ½-inch Intalox saddle

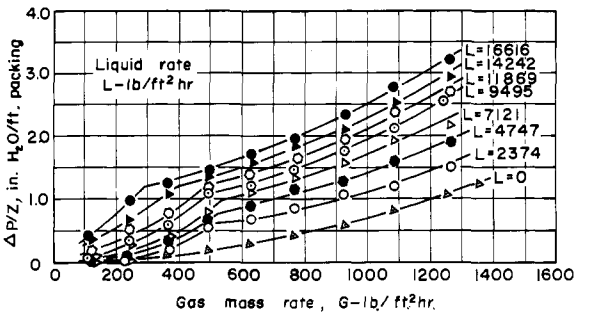

Figure 6. Pressure drop data; 1-inch Raschig rings

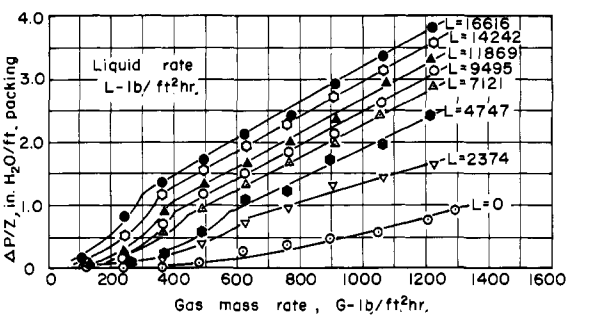

Figure 7. Pressure drop data; 1-inch Intalox saddles

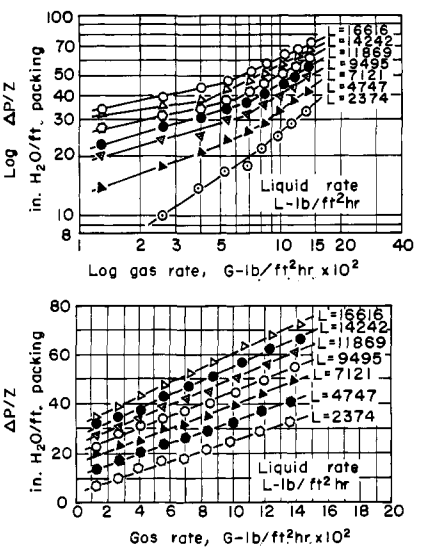

Figure 8. Pressure drop data comparison of logarithmic vs. arithmetic data plots

Table II. Empirical Constants for the Pressure Drop Equation

$\Delta P = a(L-b)^c + d\,10^{eL}G$

Air–Calcium Chloride Solution System, 39 wt. % $CaCl_2$

ΔP = Differential pressure drop, inches water/ft. packing
L = Liquid mass flow rate, lb./sq. ft. hr.
G = Gas mass flow rate, lb./sq. ft. hr.

Packing Type	a	b	c	d	$e \times 10^5$
¼-inch Raschig rings	0.0926	1,780	0.601	0.01940	1.130
½-inch Raschig rings	0.00487	2,209	0.785	0.00673	0.866
½-inch Berl saddles	0.00286	2,333	0.807	0.00409	0.936
½-inch Intalox saddles	0.00135	2,253	0.896	0.00443	1.421
1-inch Raschig rings	0.0000396	7,046	1.000	0.00133	1.433
1-inch Intalox saddles	0.0000776	12,419	1.00	0.00243	0.436

coordinates. At these points, the constant liquid rate curves seemingly change the slope. Figure 8 is a comparison of the Δ P *vs.* G for ¼-inch Raschig rings plotted on arithmetical and also on logarithmic graphs. The nature of the data with a non zero intercept produces the askewed log-log curve, indicating, erroneously, the presence of more than one flow region.

LITERATURE CITED

(1) Dodds, W.S., Ph.D. dissertation, Northwestern University Evanston, Ill., 1953.
(2) Doss, W.S., Stutzman, L.R., Sollami, B.J., McCarter, R.J., *A.I.Ch.E. J.* **6**, 390 (1960).
(3) Larkin, R.P., Ph.D. dissertation, University of Michigan, Ann Arbor, Mich., 1959.
(4) Leva, Max, United States Stoneware Co., Akron, Ohio, Bull. TP 54, 1951.
(5) Martinelli, R.C., Boelter, L.M.K., Taylor, T.H.M., Thompson, E.G., Morrin, E.H., *Trans. A.S.M.E.* **66**, 139 (1944).
(6) McIlvroid, H.G., Ph.D. dissertation, Carnegie Inst. Technol., Pittsburgh, Pa., 1956.
(7) Wen, C.Y., O'Brien, W.S., Fan, Liang-tseng, J. CHEM. ENG. DATA 8, this issue, 1963.

RECEIVED for review April 23, 1962. Accepted August 24, 1962.

Material (Table I) supplementary to this article has been deposited as Document No. 7379 with the ADI auxiliary Publication Project, Photoduplication Service, Library of Congress, Washington 25, D. C. A copy may be secured by citing the document number and by remitting $1.25 for photoprints or $1.25 for 35 mm. microfilm. Advance payment is required. Make checks or money orders payable to Chief, Photoduplication Service, Library of Congress.

Thermal Decomposition of Sodium Carbonate Solutions

ARTHUR M. THOMAS, Jr.
Esso Research and Engineering Co. Linden, N. J.

A high pressure autoclave was used to study the thermal decomposition of sodium carbonate to form sodium hydroxide in water solution. Solutions containing initially 1 wt. %, 2.5 wt. %, and 5 wt. % sodium carbonate were stripped with saturated steam at rates of 500 and 1000 ml./hr. Temperatures ranged from 410° F. to 594° F. at the corresponding equilibrium pressures. Conversion rate decreased as sodium carbonate concentration decreased at the same steaming rate and temperature. Rate of conversion also decreased as steaming rate was lowered. Higher temperatures resulted in higher absolute levels of conversion up to a maximum at 550° F. (1,000 p.s.i.g.) for 2.5 wt. % sodium carbonate solutions. Conversion of sodium carbonate to sodium hydroxide in water is limited by reaction equilibrium. Equilibrium data were obtained for the range of conditions studied.

PETROLEUM REFINERS are often faced with the problem of disposing of spent caustic solutions resulting from sweetening operations on petroleum fractions. Discard of such material into natural waters causes severe pollution problems and hence is subject to governmental restrictions. A particularly troublesome problem arises in disposing of caustic that has been used to wash some virgin and/or cracked distillates. A spent caustic from this type of operation contains naphthenic and phenolic compounds as well as sulfides and heavier mercaptans. The simple processes such as air blowing (*4*) or steam stripping are not applicable to spent caustic containing these materials. Because these compounds are difficult to remove, a complicated disposal process is needed.

Neutralization of the spent caustic with a weak acid, such as CO_2, will release the dissolved (or reacted) naphthenates and phenolates. Carbonation at atmospheric pressure converts sulfides to colloidal sulfur and sodium carbonate, and converts mercaptides, phenolates, and naphthenates to free organic compounds and sodium carbonate.